Organic & Biomolecular Chemistry

RSC Publishing

PAPER

View Article Online
View Journal | View Issue

The water-soluble argentivorous molecule: Ag^+–π interactions in water†

Cite this: *Org. Biomol. Chem.*, 2013, **11**, 4265

Yoichi Habata,*[a,b] Yoko Okeda,[b] Mari Ikeda[a,b] and Shunsuke Kuwahara[a,b]

Received 21st January 2013,
Accepted 2nd May 2013

DOI: 10.1039/c3ob40125a

www.rsc.org/obc

Ag^+–π interactions between Ag^+ ions and a water-soluble tetra-armed cyclen bearing aromatic side-arms (tetracesium 4,4′,4″,4‴-((1,4,7,10-tetraazacyclododecane-1,4,7,10-tetrayl)tetrakis(methylene))tetrabenzoate, Cs_4**L**) are reported. The structure of the Ag^+ complex with Cs_4**L** was examined using cold ESI-MS, and ^{1}H NMR and UV spectroscopies. It is found that when it forms Ag^+ complexes in water, Cs_4**L** behaves like an insectivorous plant (Venus flytrap).

Introduction

Metal-cation–π interactions have been a topic of much interest in the past decade.[1–5] However, reports of metal-cation–π interactions in water are very rare. Only one case of metal-cation–π interactions in water has been reported, *i.e.*, between *p*-sulfonatocalix[4]arene and several metal cations.[6] In that system, Tl^+–π interactions were suggested, but no specific metal-cation–π interactions were reported for Na^+ and Ag^+ ions.[6] It was also reported that Ag^+–π interactions are very difficult in water, because Ag^+ ions are much more hydrated than other monovalent cations. Recently, we reported that tetra-armed cyclens with aromatic side-arms behave like an insectivorous plant (Venus flytrap) when they form complexes with Ag^+ ions, *i.e.*, the aromatic side-arms cover the Ag^+ ions incorporated in the ligand cavities, and no conformational changes are observed when other metal cations are added.[7] We called the tetra-armed cyclen an "argentivorous molecule".[8] Here, we report Ag^+–π interactions in water with a water-soluble tetra-armed cyclen (Cs_4**L**).

Results and discussion

Cs_4**L** was prepared *via* two routes, as shown in Scheme 1: one route is *via* a tetra-armed cyclen bearing methyl benzoate groups in the side-arms (**3**) and another is *via* a tetra-armed cyclen bearing bromophenyl groups in the side-arms (**5**).

Structures of **3** and **5** were confirmed by ^{1}H and ^{13}C NMR spectroscopies, elemental analysis, and X-ray crystallography (Fig. S1, S2, S5, S6, S20–24, and Table S5 in the ESI†). As we previously reported, the protons at the 2′-/6′-positions of the aromatic side-arms shifted to a higher field in the ^{1}H NMR titration experiments, when the side-arms cover the Ag^+ ion incorporated in the cavity ligand. As shown in Fig. S22 in the ESI,† the 2′-/6′-protons (H_b protons) of the aromatic side-arms in **3** shifted to a higher field by *ca.* 0.87 ppm. On the other hand, the 3′-/5′-protons (H_a protons) shifted to a lower field by *ca.* 0.08 ppm.

The X-ray structure of the **3**–$AgCF_3SO_3$ complex (Fig. 1) shows that the hydrogens at the 2′-/6′- and 3′-/5′-positions are located in the shielded and deshielded areas of the next aromatic side-arms. The C7–Ag1 distance is 3.326 Å. The distance is comparable with those of anthracene-cryptand–Ag^+ and anthracene-diphosphine–Ag^+ systems.[9] The X-ray structure suggests that the Ag^+ ions interact with the aromatic side-arms with η^2-hapticity. The X-ray results support the ^{1}H NMR

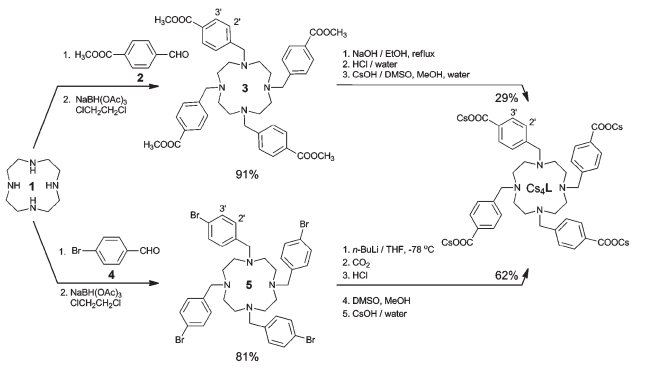

Scheme 1 Synthetic procedure.

[a]*Department of Chemistry, Faculty of Science, Toho University, 2-2-1 Miyama, Funabashi, Chiba 274-8510, Japan. E-mail: habata@chem.sci.toho-u.ac.jp; Fax: +81 47 472 4322*
[b]*Research Centre for Materials with Integrated Properties, Toho University, 2-2-1 Miyama, Funabashi, Chiba 274-8510, Japan*

†Electronic supplementary information (ESI) available: ^{1}H and ^{13}C NMR spectra of compounds, titration experiments, X-ray structures (PDF). CCDC 919399–919402. For ESI and crystallographic data in CIF or other electronic format see DOI: 10.1039/c3ob40125a

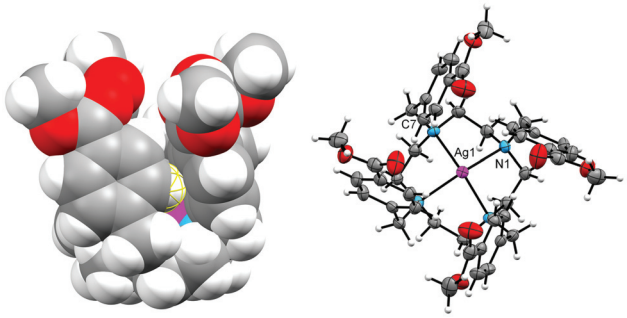

Fig. 1 Spacefilling diagram (left, side view) and ORTEP diagram (right, top view) of **3**–$AgCF_3SO_3$ (left). The CF_3SO_3 anion is omitted. Meshed hydrogens are the protons at the 2′- and 6′-positions of the side-arms.

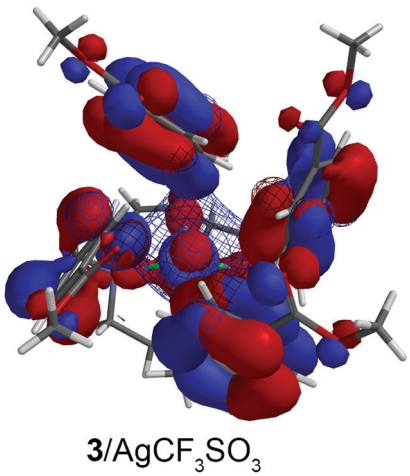

Fig. 2 The LUMO and HOMOs calculated by the DFT method [B3LYP/3-21G(*)] using the X-ray structures of the Ag^+ complex with **3** (isosurface value is 0.032 au). LUMO[+4] (mesh) and HOMO[−11], HOMO[−12], HOMO[−12], and HOMO[−14] (solid).

titration experiments. Fig. 2 shows the LUMO and HOMOs calculated by the DFT method [B3LYP/3-21G(*)] using the X-ray structures of the Ag complex with **3**. The result indicates the interactions between LUMO of Ag^+ and HOMOs and the aromatic side-arms.

The sodium salt of the ligand (Na_4**L**) was very difficult to purify, because Na_4**L** and NaOH precipitate together. On the other hand, the cesium salt of the ligand (Cs_4**L**) was easy to purify by recrystallization from a mixture of DMSO and water. We, therefore, used cesium salt of the ligand. The structure of Cs_4**L** was confirmed by ^1H, ^{13}C NMR, and IR spectroscopies, cold ESI-MS, elemental analysis, and X-ray crystallography (Fig. S3, S4, S8–S10, and Table S1 in the ESI†).

As shown in Fig. 3 (and Fig. S8 in the ESI†), two water and two DMSO molecules bind to the Cs^+ ions in the Cs_4**L**. The Cs–O distances are in the range of 3.050–3.443 Å and are comparable with the typical Cs–O distances of cesium benzoate derivatives.[10] The presence of water and DMSO molecules was also observed in the ^1H NMR and IR spectra (Fig. S3 and S10 in the ESI†) and elemental analyses. In cold ESI-MS, the

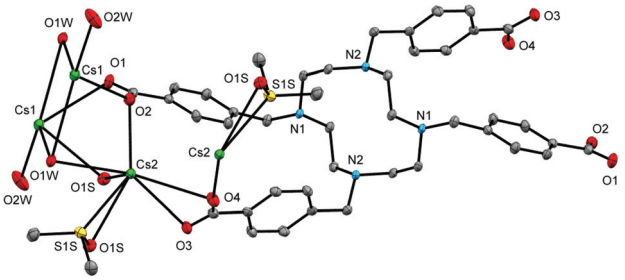

Fig. 3 ORTEP diagram of Cs_4**L**. Two water and two DMSO molecules bind to cesium ions.

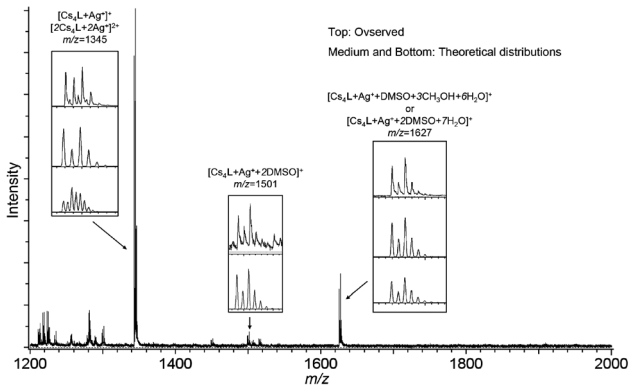

Fig. 4 Cold ESI-MS of a 1 : 1 mixture of Cs_4**L** and $AgCF_3SO_3$ at 298 K (in H_2O–CH_3OH (1/7, v/v)).

fragment ion peaks arising from $[Cs_4\mathbf{L} + H^+]^+$ and $[Cs_4\mathbf{L} + Cs^+]^+$ were observed.

To examine the structure of the Ag^+ complex with Cs_4**L** including DMSO and water molecules, cold ESI-MS of a 1 : 1 mixture of Cs_4**L** and $AgCF_3SO_3$ was conducted in a mixture of H_2O–CH_3OH (1/7, v/v). Cold ESI-MS is an excellent tool for confirming the presence of unstable species and/or solvated species.[11] The fragment ion peaks arising from $[Cs_4\mathbf{L} + Ag^+]^+$, $[2Cs_4\mathbf{L} + 2Ag^+]^{2+}$, $[Cs_4\mathbf{L} + Ag^+ + 2DMSO]^+$, and $[Cs_4\mathbf{L} + Ag^+ + DMSO + 3CH_3OH + 6H_2O]^+$ (or $[Cs_4\mathbf{L} + Ag^+ + 2DMSO + 7H_2O]^+$) were observed at m/z = 1345, 1349, 1501, and 1627, respectively (Fig. 4). It is important to note that the fragment ion peaks at m/z = 1345–1349 are overlapped by the $[Cs_4\mathbf{L} + Ag^+]^+$ and $[2Cs_4\mathbf{L} + 2Ag^+]^{2+}$ ions. The patterns of the fragment ion peaks agree with the theoretical distributions (see Fig. S11a and 11b in the ESI†). The mass spectrometry data suggest that the $AgCF_3SO_3$ complex with Cs_4**L** is a 1 : 1 complex.

Titration experiments using ^1H NMR were carried out in D_2O. We reported that[7] unusual higher-field shifts of the protons at the 2′-/6′-positions in the aromatic side-arms are observed upon the addition of equimolar amounts of Ag^+ ions when the aromatic side-arms cover the Ag^+ ions incorporated in the ligand cavities. If the aromatic side-arms of Cs_4**L** cover the Ag^+ ions in water, the protons at the 2′-/6′-positions in the aromatic side-arms should shift to a higher field because the 2′-/6′-protons are located in the shielded area of the next

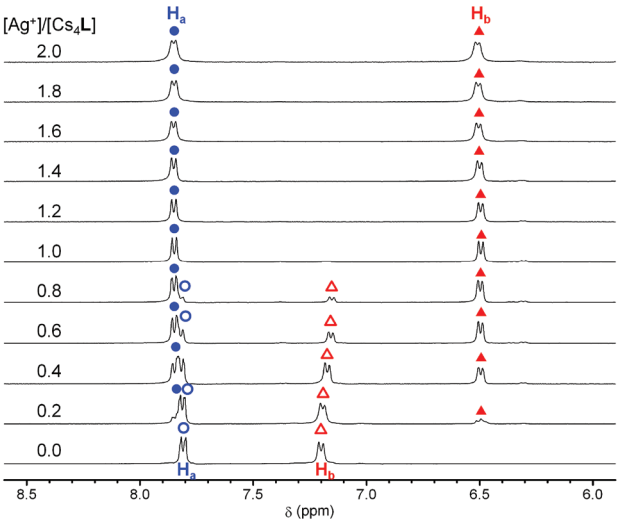

Fig. 5 $AgCF_3SO_3$-induced ^1H NMR spectral changes (in D_2O). H_a (uncomplexed, blue ○; complexed, blue ●) and H_b (uncomplexed, red △; complexed, red ▲) mean the protons at 3′-/5′- and 2′-/6′-positions in the side-arms, respectively (298 K).

aromatic side-arm in solution. Fig. 5 shows the results of the $AgCF_3SO_3$-induced ^1H NMR titration experiments in D_2O (aromatic region). Upon the addition of equimolar amounts of Ag^+ ions, as the intensities of the doublet at δ 7.8 ppm and the doublet at δ 7.2 ppm decrease, the intensities of the doublet at δ 7.85 ppm and the doublet at δ 6.5 ppm increase. The chemical shift changes stopped at a ratio of 1 : 1. When $AgPF_6$ and $AgNO_3$ were used instead of $AgCF_3SO_3$, the protons at the 2′-/6′-positions shifted by *ca.* −0.7 ppm (see Fig. S13 and S14, and Table S2 in the ESI†). As presented above, the X-ray structure of the **3**–$AgCF_3SO_3$ complex indicates that the H_a protons are located in the deshielded area of the next aromatic side-arms. The H_a protons in the Cs_4**L**–Ag^+ complex, therefore, would be also shifted to a lower field. The ^1H NMR spectra show that (i) higher-field shifts (*ca.* −0.7 ppm) of the protons at the 2′-/6′-positions are observed in water and (ii) Cs_4**L** forms a 1 : 1 complex with Ag^+ ions. These ^1H NMR titration experiments strongly support that the aromatic side-arms in Cs_4**L** cover the Ag^+ ions incorporated in the ligand cavity as we expected. On the other hand, no spectral changes were observed upon the addition of equimolar amounts of Li^+, Na^+, K^+, Mg^{2+}, Ca^{2+}, Sr^{2+}, Ba^{2+}, Co^{2+}, Ni^{2+} ions (Table S3 in the ESI†). When $Pb^{2+}$and Zn^{2+} ions were added, slight changes were observed. [Fig. S17 and S18 in the ESI† show Pb^{2+} and Zn^{2+}-ions-induced ^1H NMR spectral changes, respectively. ^1H–^1H HOHAHA NMR (Fig. S19†) was used to assign the H_a and H_b protons in a 1 : 0.5 mixture of Cs_4**L** and $Pb(NO_3)_2$.]

Titration experiments using UV spectra were carried out to confirm the Ag^+–π interactions in water. Fig. 6 shows the Ag^+-ion-induced UV spectral changes of Cs_4**L**. A decrease and an increase in the absorbance at 230 nm (λ_{max}) and shorter wavelengths were observed, respectively, with an isosbestic point at 220 nm, upon the addition of Ag^+ ions. An inflection point was observed at 1.0 (=[Ag^+]–[Cs_4**L**]), showing a 1 : 1 complex.

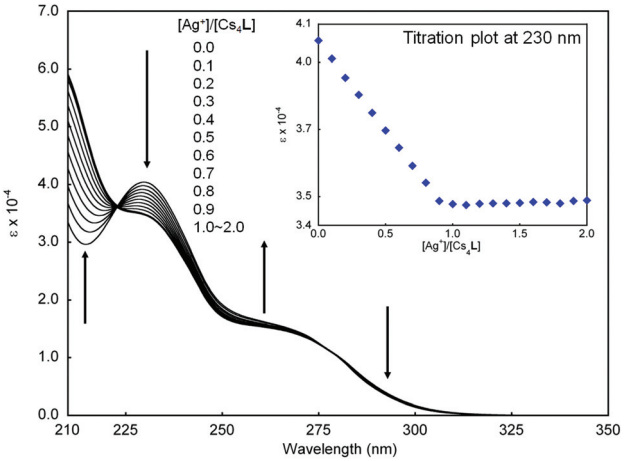

Fig. 6 $AgCF_3SO_3$-induced UV spectral changes and titration plots at 230 nm (in water). [Cs_4**L**] = 5.0 × 10^{-5} mol L^{-1}.

Nonlinear least-squares analyses of the titration profiles (absorbance *versus* equivalents of Ag^+ added, see Fig. S25 in the ESI†) clearly indicated the formation of a 1 : 1 complex, and allowed us to estimate the association constants defined as eqn (1).[12]

$$Cs_4\mathbf{L} + Ag^+ \leftrightarrow [Cs_4\mathbf{L}\text{–}Ag^+]$$

$$K = [Cs_4\mathbf{L}\text{–}Ag^+]/[Cs_4\mathbf{L}][Ag^+] \quad (1)$$

From the UV spectral data, the log K value of the complex was estimated to be *ca.* 10.9 (Fig. S26 in the ESI†). This result strongly supports Ag^+–π interactions between the aromatic side-arms and Ag^+ ions in water.

The complexing properties of Cs_4**L** toward several metal ions were examined based on metal-ion-induced UV spectral changes in water. When equimolar amounts of Ag^+ were added, significant spectral changes were observed, as shown in Fig. 7 and 8, whereas no spectral changes were observed upon the addition of equimolar amounts of Li^+, Na^+, K^+, Mg^{2+}, Ca^{2+}, Sr^{2+}, Ba^{2+}, Co^{2+}, Ni^{2+}, Zn^{2+}, and Cd^{2+} ions. In contrast, a

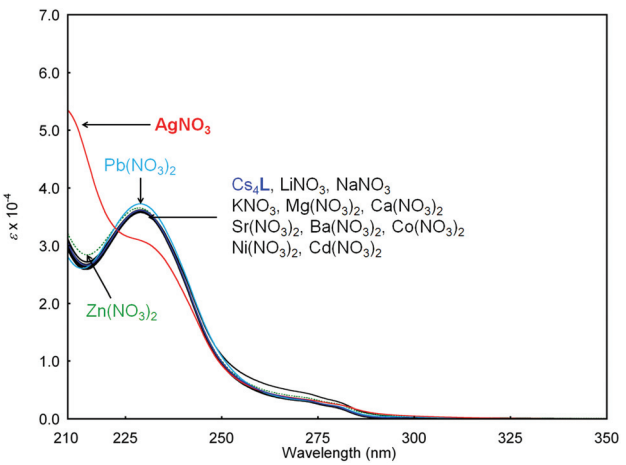

Fig. 7 Metal-ion-induced UV spectral changes (in water).

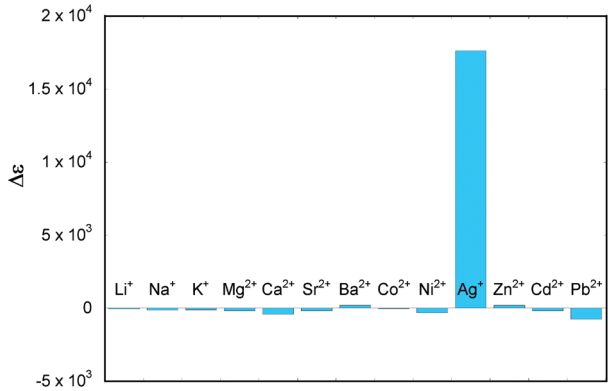

Fig. 8 Changes of ε ($\Delta\varepsilon$) at 215 nm upon the addition of various metal cations ([cations] : [Cs_4**L**] = 1 : 1).

slight UV spectral change was observed on the addition of Pb^{2+} ions. To investigate the spectral change upon the addition of Pb^{2+} ions, Pb^{2+}-induced UV spectral changes were observed using a mixture of cyclen and cesium 4-methylbenzoate (1/4, v/v) or cesium 4-methylbenzoate as ligands (Fig. S15 and S16 in the ESI†). In both cases, an increase at λ_{max} (230 nm) was observed upon the addition of Pb^{2+} ions. It is well known that carboxylate binds to Pb^{2+} ions.[13] The UV spectral changes in Cs_4**L** resulted from the binding of the COO^- groups in the side-arms to Pb^{2+} ions. Two types of proton signals at the 2′-/6′- and 3′-/5′-positions appeared in the Pb^{2+}-induced ^{1}H NMR titration experiments (Fig. S17 in the ESI†). The ^{1}H NMR data strongly support binding of the COO^- groups. These results indicate that sensing using UV spectroscopy with Cs_4**L** provides Ag^+ selectivity.

Conclusions

In conclusion, we have demonstrated that a water-soluble tetra-armed cyclen with aromatic side-arms behaves like an insectivorous plant (Venus flytrap) when forming Ag^+ complexes. We confirmed that the conformational changes are the result of Ag^+–π interactions between the Ag^+ ions and the aromatic side-arms in water. The unique property of this water-soluble argentivorous molecule shows an application for new supramolecular systems of Ag^+–π interactions (Fig. 9).

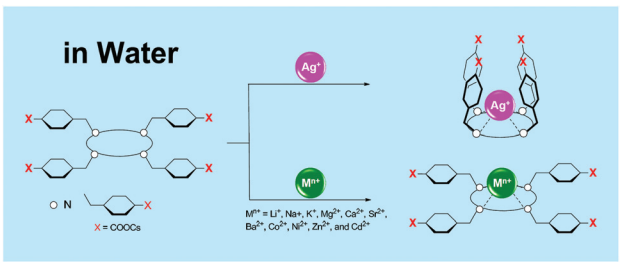

Fig. 9 Image of the water-soluble argentivorous molecule.

Experimental

Melting points were obtained with a Mel-Temp capillary apparatus and not corrected. FAB-MS was performed using a JEOL 600 H spectrometer. ^{1}H NMR spectra were measured in $CDCl_3$ on a JEOL ECP400 (400 MHz) spectrometer. Cold ESI-MS were recorded on a JEOL JMS-T100CS spectrometer. UV-vis spectra were recorded on a JASCO V-650 spectrometer. CD spectra were recorded on a JASCO J-820 spectrometer. Cyclen was purchased from Macrocyclics. All reagents were standard analytical grade and were used without further purification.

Synthesis of tetramethyl 4,4′,4″,4‴-[1,4,7,10-tetraazacyclododecane-1,4,7,10-tetrayltetrakis(methylene)]-tetrabenzoate (3)

After a mixture of cyclen (**1**) (0.268 g, 1.56 mmol), methyl 4-formylbenzoate (**2**) (2.23 g, 13.6 mmol), and $NaBH(OAc)_3$ (2.92 g, 13.8 mmol) in 1,2-dichloroethane (15 mL) was stirred for 5 days at rt under a nitrogen atmosphere, saturated aqueous $NaHCO_3$ was added. The organic layer was separated, and the aqueous layer was extracted with $CHCl_3$ (100 mL × 3). The combined organic layer was washed with water, dried over Na_2SO_4, and concentrated. The residue was recrystallized from acetonitrile (5 mL) to give **3**.

Yield 1.02 g (91%). Mp. 196.0–197.2 °C (dec.). FAB-MS (matrix DTT : TG = 1 : 1, *m*/*z*), 766 ([M + 1]$^+$, 100%); ^{1}H NMR ($CDCl_3$) 7.92 (d, *J* = 8.2 Hz, 8H), 7.39 (d, *J* = 8.2 Hz, 8H), 3.92 (s, 12H), 3.44 (s, 8H), 2.66 (s, 16H). ^{13}C NMR ($CDCl_3$) 167.3, 145.7, 129.7, 129.0, 128.9, 60.1, 53.6, 52.2. Anal. Calcd for $C_{44}H_{52}N_4O_8$: C, 69.09; H, 6.85; N, 7.32. Found: C, 68.85; H, 6.74; N, 7.16.

Synthesis of tetracesium 4,4′,4″,4‴-(1,4,7,10-tetraazacyclododecane-1,4,7,10-tetrayltetramethanediyl)-tetrabenzoate (Cs_4L)

After a mixture of **3** (0.0377 g, 0.0493 mmol) and powdered NaOH (0.180 g, 4.50 mmol) in ethanol (55 mL) was refluxed for 1 day under a nitrogen atmosphere, solvent was evaporated *in vacuo*. The residue was recrystallized from methanol (15 mL) to give the crude product of Na_4L including NaOH. The solid was dissolved in water and then 10 mL of aqueous HCl (2 mol L^{-1}) was added. The residual precipitate was washed with $CHCl_3$ (10 mL) and water (10 mL) to give H_4L·4HCl as white powders. After H_4**L**·4HCl was dried *in vacuo*, the powders were dissolved in 10 mL of DMSO, and then a saturated aqueous CsOH solution was added until the pH reaches 8 to give Cs_4**L** as white powders.

Yield 0.0449 g (29%). Mp. 224 °C (dec.). Cold ESI-MS (H_2O–CH_3OH = 1 : 7, *m*/*z*), 1237 [Cs_4**L** + H^+]$^+$), 1369 ([Cs_4**L** + Cs^+]$^+$). ^{1}H NMR (D_2O) 7.79 (d, *J* = 8.0 Hz, 8H), 7.19 (d, *J* = 8.0 Hz, 8H), 3.61 (s, 8H), 2.83 (s, 16H). ^{13}C NMR (D_2O) 176.3, 136.8, 131.1, 130.1, 59.5, 49.0, 39.9. IR (KBr disk, cm^{-1}) 3413, 2928, 2791, 1597, 1550, 1397, 1012. Anal. Calcd for $C_{40}H_{40}Cs_4N_4O_8$ + 2DMSO + 4H_2O: C, 36.08; H, 4.13; N, 3.83. Found: C, 36.28; H, 4.11; N, 3.77.

Synthesis of 1,4,7,10-tetrakis(4-bromobenzyl)-1,4,7,10-tetraazacyclododecane (5)

After a mixture of cyclen (**1**) (0.346 g, 2.01 mmol) and 4-bromobenzaldehyde (**4**) (3.32 g, 17.9 mmol) in 1,2-dichloroethane (28 mL) was stirred for 2 hours at rt under a nitrogen atmosphere, $NaBH(OAc)_3$ (2.92 g, 13.8 mmol) was added and stirred for 1 day under a nitrogen atmosphere. Saturated aqueous $NaHCO_3$ was added to the reaction mixture and then the residue was extracted with $CHCl_3$ (100 mL × 3). The organic layer was separated and combined. The organic layer was washed with water, dried over Na_2SO_4, and concentrated *in vacuo*. The residue was recrystallized from acetonitrile (5 mL) to give **5** as white crystals.

Yield 1.38 g (81%). Mp. 184.8–186.0 °C. FAB-MS (matrix *m*-NBA, *m*/*z*) 845 ($[M - 3]^+$, 4%), 847 ($[M - 1]^+$, 12%), 849 ($[M + 1]^+$, 19%), 851 ($[M + 3]^+$, 13%), 853 ($[M + 5]^+$, 4%). ^{1}H NMR ($CDCl_3$) 7.37 (d, J = 8.2 Hz, 8H), 7.16 (d, J = 8.2 Hz, 8H), 3.33 (s, 8H), 2.61 (s, 16H). ^{13}C NMR ($CDCl_3$) 139.2, 131.4, 130.9, 120.8, 59.8, 53.4. Anal. Calcd for $C_{36}H_{40}Br_4N_4$: C, 50.97; H, 4.75; N, 6.60. Found: C, 50.88; H, 4.75; N, 6.35.

Synthesis of tetracesium 4,4′,4″,4‴-((1,4,7,10-tetraazacyclododecane-1,4,7,10-tetrayl)tetrakis(methylene))-tetrabenzoate (Cs_4**L**)

n-Butyl lithium (1.6 mol L^{-1} in hexane, 3.0 mL) was added to **5** (0.846 g, 0.997 mmol) in absolute THF (60 mL) at −78 °C under an argon atmosphere. After dry ice (>44 mg) was added to the reaction mixture, the flask was stirred for 1 h at rt. Water (10 mL) and aqueous HCl (2 mol L^{-1}, 10 mL) were added to the reaction mixture, and then the residual precipitate was washed with $CHCl_3$ (15 mL) and water (15 mL) to give H_4**L**·4HCl as white powders. After H_4**L**·4HCl was dried *in vacuo*, the powders were dissolved in a mixture of DMSO (15 mL) and methanol (150 mL). To the solution was added dropwise a saturated aqueous CsOH solution until the pH reaches 8 to give Cs_4**L** as white powders.

Yield 0.899 g (62%).

Synthesis of cesium 4-methylbenzoate

A saturated aqueous CsOH solution was added dropwise to 4-methylbenzoic acid (0.96 g, 5.07 mmol) in methanol (70 mL) until the pH reaches 8. The residual precipitate was washed with methanol.

Yield 70%. ^{1}H NMR (D_2O) 7.76 (d, J = 8.2 Hz, 2H), 7.28 (d, J = 8.2 Hz, 2H), 2.36 (s, 3H). Anal. Calcd for $C_8H_7O_2Cs + 1.5H_2O$: C, 34.13; H, 3.04. Found: C, 34.29; H, 3.24.

Preparation of the 3–$AgCF_3SO_3$ complex

Compound **3** (9.20 mg, 0.025 mmol) in chloroform (1 mL) was added to $AgCF_3SO_3$ (15.0 mg, 0.025 mmol) in methanol (1 mL). Acetonitrile and 1,2-dichloroethane (0.5 mL) were added to the mixture. Crystals were obtained quantitatively on evaporation of the solvent.

Anal. Calcd for $C_{45}H_{52}N_4AgF_3O_{11}S$: C, 52.89; H, 5.13; N, 5.48. Found: C, 53.22; H, 5.24; N, 5.33. ^{1}H NMR ($CDCl_3$–CD_3OD = 0.75/0.005, v/v) 7.99 (d, J = 7.9 Hz, 8H), 6.52 (d, J = 7.9 Hz, 8H), 4.03 (s, 12H), 3.16 (broad-s, 16H), 2.45 (broad-s, 8H). ^{13}C NMR ($CDCl_3$–CD_3OD = 0.75/0.005, v/v) 166.2, 143.4, 130.8, 130.6, 129.7, 58.9, 52.6, 50.1. The ^{13}C signals of the CF_3SO_3 anion were not observed under the condition.

^{1}H NMR titration experiments

^{1}H NMR titration experiments were carried out at 298 K by the addition of 0.2–2.0 (or 0.5–2.0) equivalents of metal salts ($LiNO_3$, $NaNO_3$, $Mg(NO_3)_2$, $Ca(NO_3)_2$, $Sr(NO_3)_2$, $Co(NO_3)_2$, $Ni(NO_3)_2$, $AgNO_3$, $AgCF_3SO_3$, $AgPF_6$, and $Zn(NO_3)_2$: 0.001 mmol μL^{-1}) in D_2O ($CDCl_3$–CD_3OD for **3**) to Cs_4**L** (0.01 mmol/0.65 mL in D_2O, $CDCl_3$–CD_3OD for **3**).

X-ray structure determination

Crystals of the Cs_4**L**, **3**, **3**–$AgCF_3SO_3$ complex, and **5** were mounted on top of a glass fiber, and data collection was performed at 100–173 K. Data were corrected for Lorentz and polarization effects, and absorption corrections were applied.[14] Structures were solved by a direct method and subsequent difference-Fourier syntheses.[15] All non-hydrogen atoms were refined anisotropically and hydrogen atoms were placed at calculated positions and then refined using $U_{iso}(H) = 1.2U_{eq}(C)$. The crystallographic refinement parameters of the complexes are summarized in Tables S1 and S4–S6 in the ESI.†

Acknowledgements

This research was supported by Grants-in-Aid (08026969 and 11011761), a High-Tech Research Center project (2005–2009), and the Supported Program for Strategic Research Foundation at Private Universities (2012–2016) from the Ministry of Education, Culture, Sports, Science and Technology of Japan, and the Futaba Memorial Foundation, for Y.H.

Notes and references

1 (*a*) G. W. Gokel, *Chem. Commun.*, 2003, 2847; (*b*) G. W. Gokel, L. J. Barbour, W. S. L. De and E. S. Meadows, *Coord. Chem. Rev.*, 2001, **222**, 127; (*c*) G. W. Gokel, W. S. L. De and E. S. Meadows, *Eur. J. Org. Chem.*, 2000, 2967.
2 A. J. Petrella and C. L. Raston, *J. Organomet. Chem.*, 2004, **689**, 4125.
3 Z. Xu, *Coord. Chem. Rev.*, 2006, **250**, 2745.
4 S. D. Zaric, *Eur. J. Inorg. Chem.*, 2003, 2197.
5 M. Munakata, L. P. Wu and G. L. Ning, *Coord. Chem. Rev.*, 2000, **198**, 171.
6 J.-P. Morel and N. Morel-Desrosiers, *Org. Biomol. Chem.*, 2006, **4**, 462.
7 (*a*) Y. Habata, M. Ikeda, S. Yamada, H. Takahashi, S. Ueno, T. Suzuki and S. Kuwahara, *Org. Lett.*, 2012, **14**, 4576; (*b*) Y. Habata, A. Taniguchi, M. Ikeda, T. Hiraoka, N. Matsuyama, S. Otsuka and S. Kuwahara, *Inorg. Chem.*,

2013, **52**, 2542; (*c*) Y. Habata, Y. Oyama, M. Ikeda and S. Kuwahara, *Dalton Trans.*, 2013, DOI: 10.1039/c3dt00034f.

8 "Argentivorous" is different from "argentophilic". "Argentophilic" is used in the sense of Ag^{+}–Ag^{+} interactions. For example, (*a*) E. C. Constable, C. E. Housecroft, P. Kopecky, M. Neuburger and J. A. Zampese, *Inorg. Chem. Commun.*, 2013, **27**, 159–162; (*b*) G.-G. Luo, D.-L. Wu, L. Liu, S.-H. Wu, D.-X. Li, Z.-J. Xiao and J.-C. Dai, *J. Mol. Struct.*, 2012, **1014**, 92–96; (*c*) R. Santra, M. Garai, D. Mondal and K. Biradha, *Chemistry*, 2013, **19**, 489–493; (*d*) G. A. Senchyk, V. O. Bukhan'ko, A. B. Lysenko, H. Krautscheid, E. B. Rusanov, A. N. Chernega, M. Karbowiak and K. V. Domasevitch, *Inorg. Chem.*, 2012, **51**, 8025–8033; (*e*) A. Stephenson and M. D. Ward, *Chem. Commun.*, 2012, **48**, 3605–3607; (*f*) J. Xu, S. Gao, S. W. Ng and E. R. T. Tiekink, *Acta Crystallogr., Sect. E: Struct. Rep. Online*, 2012, **68**, m639–m640; (*g*) J. Xu, S. Gao, S. W. Ng and E. R. T. Tiekink, *Acta Crystallogr., Sect. E: Struct. Rep. Online*, 2012, **68**, m639–m640; (*h*) G. Yang, P. Baran, A. R. Martinez and R. G. Raptis, *Cryst. Growth Des.*, 2013, **13**, 264–269.

9 (*a*) F. B. Xu, L. H. Weng, L. J. Sun and Z. Z. Zhang, *Organometallics*, 2000, **19**, 2658; (*b*) F. Li, Q. Xu, L. Wu, X. Leng, Z. Li, Z. Zeng, Y. L. Chow and Z. Zhang, *Organometallics*, 2003, **22**, 633.

10 (*a*) D. Braga, S. D'Agostino and F. Grepioni, *CrystEngComm*, 2011, **13**, 1366; (*b*) D. Braga, S. D'Agostino, M. Polito, K. Rubini and F. Grepioni, *CrystEngComm*, 2009, **11**, 1994; (*c*) F. Wiesbrock and H. Schmidbaur, *Inorg. Chem.*, 2003, **42**, 7238; (*d*) D. Luehrs and K. Bowman-James, *J. Mol. Struct.*, 1994, **321**, 251; (*e*) N. Kasuga, S. Nakahama, K. Yamaguchi, Y. Ohashi and K. Hori, *Bull. Chem. Soc. Jpn.*, 1991, **64**, 3548.

11 (*a*) S. Sakamoto, T. Imamoto and K. Yamaguchi, *Org. Lett.*, 2001, **3**, 1793; (*b*) M. Fujita, F. Ibukuro, K. Yamaguchi and K. Ogura, *J. Am. Chem. Soc.*, 1995, **117**, 4175; (*c*) Y. Sei, K. Shikii, S. Sakamoto, M. Kunimura, T. Kobayashi, H. Seki, M. Tashiro, M. Fujita and K. Yamaguchi, *Bunseki Kagaku*, 2004, **53**, 457.

12 R. Gomes, A. J. Parola, F. Bastkowski, J. Polkowska and F. Klärner, *J. Am. Chem. Soc.*, 2009, **131**, 8922.

13 For example, (*a*) X. Li, *Acta Crystallogr., Sect. E: Struct. Rep. Online*, 2006, **62**, m2467; (*b*) H. Sadeghzadeha and A. Morsali, *J. Coord. Chem.*, 2010, **63**, 713; (*c*) J. Shi, J. Ye, T. Song, D. Zhang, K. Ma, J. Ha, J. Xu and P. Zhang, *Inorg. Chem. Commun.*, 2007, **10**, 1534.

14 G. M. Sheldrick, *Program for adsorption correction of area detector frames*, Bruker AXS, Inc., Madison, WI, 1996.

15 *SHELXTLTM, version 5.1*, Bruker AXS, Inc., Madison, WI, 1997.

